

Electronic Supplementary Information

Cobalt-doping in Hierarchical Ni₃S₂ Nanorod Arrays Enables High Areal Capacitance

Qiang Chen,^{a, b, ‡} Jialun Jin,^{a, ‡} Zongkui Kou,^b Jiangmin Jiang,^b YuluFu,^{a, b} Ziang Liu,^a

Liang Zhou,^{a, c *} and Liqiang Mai^{a, c}

^aState Key Laboratory of Advanced Technology for Materials Synthesis and Processing, Wuhan University of Technology, Wuhan 430070, China.

^bDepartment of Materials Science and Engineering, National University of Singapore, Singapore 117574, Singapore.

^cFoshan Xianhu Laboratory, Foshan 528216, Guangdong, China

E-mail: liangzhou@whut.edu.cn (L. Zhou).

[‡] These authors contribute equally to this work.

Calculations:

1. Co-Ni₃S₂ Electrode:

The areal capacitances of electrodes were measured by galvanostatic charge/discharge method according to the following equation:

$$C_a = \frac{I \times \Delta t}{\Delta V \cdot S} \quad (1)$$

where C_a (F cm⁻²) is the areal capacitance, I (A) is the constant discharging current, Δt is the discharging time, ΔV (V) is the potential window, and S (cm²) is the surface area.

2. Co-Ni₃S₂//FeOOH HSCs:

The areal capacitance (C_s) of the Co-Ni₃S₂//FeOOH HSCs was calculated from the slope of the discharge curve using the following equations:

$$C_s = \frac{I \times \Delta t}{S \times \Delta V} \quad (2)$$

where C_s (F cm⁻²) is the areal capacitance, I (A) is the applied current, S (cm²) is the volume of the whole device (The area and thickness of the Co-Ni₃S₂//FeOOH HSCs device are about 0.5 cm² and 0.1 cm, respectively), Δt (s) is the discharging time, ΔV (V) is the voltage window. It is worth mentioning that the volumetric capacitances were calculated based on the volume of the whole device. This includes the volume of electrode and the separator with electrolyte.

The time constant was calculated from the following equation:

$$\tau_0 = 1/f_0 \quad (3)$$

where τ_0 (s) is the time constant, f_0 (Hz) is the characteristic frequency at the phase angle of -45° .

Areal energy density, equivalent series resistance and power density of the devices

were obtained from the following equations:

$$E = \frac{1}{3600 \times 2} C_s \times \Delta V^2 \quad (4)$$

$$P = \frac{3600E}{\Delta t} \quad (5)$$

where E (Wh cm⁻²) is the energy density, C_s is the volumetric capacitance obtained from Equation (2) and ΔV (V) is the voltage window. P (W cm⁻²) is the power density.

3. Balance the charge of electrodes in HSCs device:

As for a SC, the charge balance will follow the relationship $q^+ = q^-$. The charge stored by each electrode depends on the capacitance (C_s), the potential range for the charge/discharge process (ΔE) and the area of the electrode (A). It follows the Equation (6):

$$q = C_s \times \Delta E \times m \quad (6)$$

In order to get $q^+ = q^-$ at 100 mV s⁻¹, the area balancing between Co-Ni₃S₂ and FeOOH electrode will be calculated as follow (7):

$$\frac{A_{Co-Ni_3S_2}}{A_{FeOOH}} = \frac{C_{A(FeOOH)} \times \Delta E_{(FeOOH)}}{C_{A(Co-Ni_3S_2)}} \approx \frac{1.2}{1} \quad (7)$$

The calculated $C_{A(FeOOH)}$ is 0.58 F cm⁻², $\Delta E_{(FeOOH)}$ is 1.2 V, $C_{A(Co-Ni_3S_2)}$ is 0.57 F cm⁻².

Therefore, the calculated areal ratio between the Co-Ni₃S₂ electrode and FeOOH electrode is about 1.2 : 1.

The electrochemical active surface area (ECSA) measurement: The capacitive current was used to determine the ECSA of the as-prepared Ni_3S_2 and $\text{Co-Ni}_3\text{S}_2$ with a scan window of 0.4 to 0.5 V vs. SCE. The current density differences at 0.45 V against the scan rate (4 to 16 mV s^{-1}) were fitted to obtain the double-layer capacitance (C_{dl}) and ECSA.

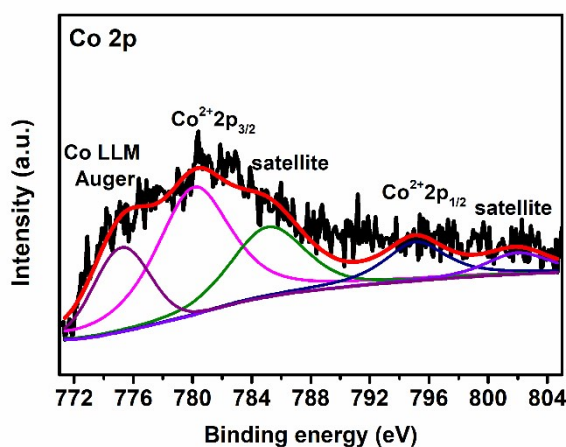


Fig. S1 Co 2p XPS spectrum of the $\text{Co-Ni}_3\text{S}_2$.

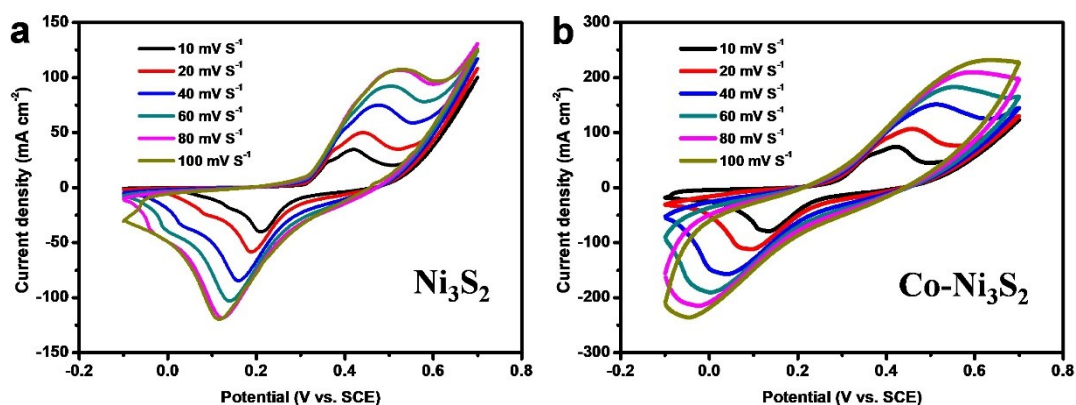


Fig. S2 CV curves of the (a) Ni_3S_2 and (b) $\text{Co-Ni}_3\text{S}_2$ at different scan rate.

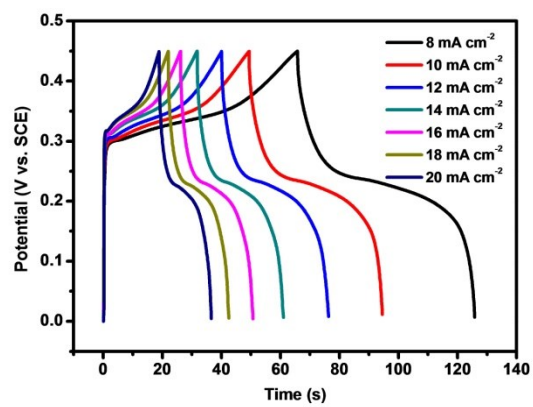


Fig. S3 GCD curves of the Ni_3S_2 nanosheets at different current densities.

Table S1. Comparison of the capacitance of Co-Ni₃S₂ nanorods with recently reported state-of-the-art supercapacitor electrode materials.

Electrode	Morphology	Current density) [mAcm ⁻²]	CP areal capacitance [Fcm ⁻²]	Scan rate [mVs ⁻¹]	CV areal capacitance [Fcm ⁻²]	Substrate	Electrolyte	Reference
Co-Ni₃S₂^{a)}	nanorods	8	3.46	10	1.81	NF	1.0 M KOH	This work
Ni₃S₂^{a)}	nanosheets	8	1.07	10	0.74	NF	1.0 M KOH	This work
Ni ₃ S ₂ @CdS ^{a)}	nanorods	8	2.92	N.A.	N.A.	NF	3.0 M KOH	S1 ¹
NiCo ₂ O ₄ @MnO ₂ ^{a)}	nanowires	8	1.91	N.A.	N.A.	NF	1.0 M NaOH	S2 ²
Ni ₃ S ₂ @β-NiS ^{c)}	nanosheets	8	2.48	N.A.	N.A.	NF	6.0 M KOH	S3 ³
Activated NF ^{a)}	thin film	8	2.04	N.A.	N.A.	NF	6.0 M KOH	S4 ⁴
Co ₃ O ₄ @C@Ni ₃ S ₂	nanoneedle	10	2.25	N.A.	N.A.	NF	3.0 M KOH	S5 ⁵
NF@NiO ^{a)}	nanosheets	8	2.01	10	1.3	NF	1.0 M KOH	S6 ⁶
NiCo-O ^{a)}	nanowires	5	2.20	N.A.	N.A.	NF	1.0 M KOH	S7 ⁷
Ni-Co-S ^{b)}	nanosheets	8	1.08	N.A.	N.A.	CC	1.0 M KOH	S8 ⁸

^{a)}vs SCE; ^{b)}vs Ag/AgCl; ^{c)} vs Hg/Hg

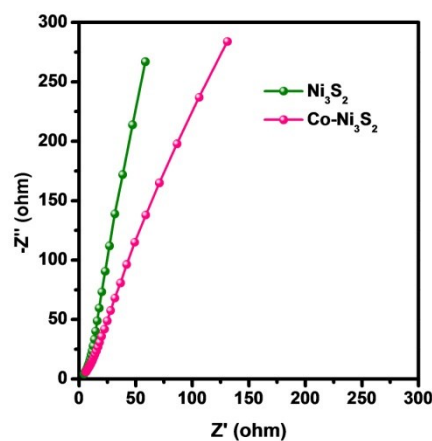


Fig. S4 Nyquist plots of Ni₃S₂ and Co-Ni₃S₂.

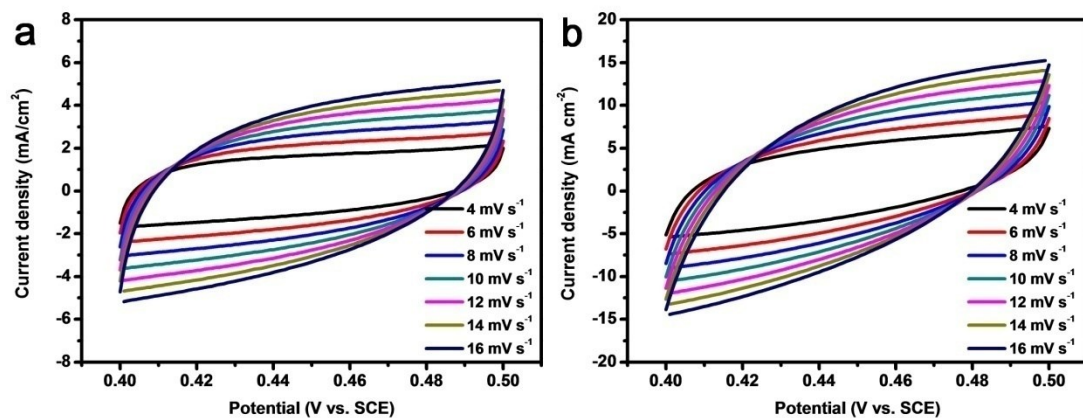


Fig. S5 CV curves in the double layer region at scan rate of 4, 6, 8 10, 12, 14, 16 mV s⁻¹ of (a) Ni₃S₂ and (b) Co-Ni₃S₂.

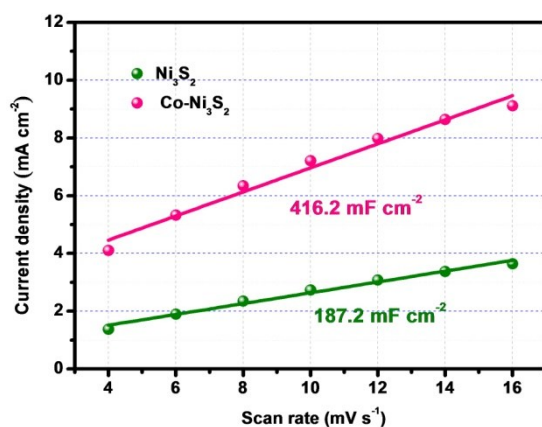


Fig.S6 Current density as a function of scan rate for Ni₃S₂ and Co-Ni₃S₂.

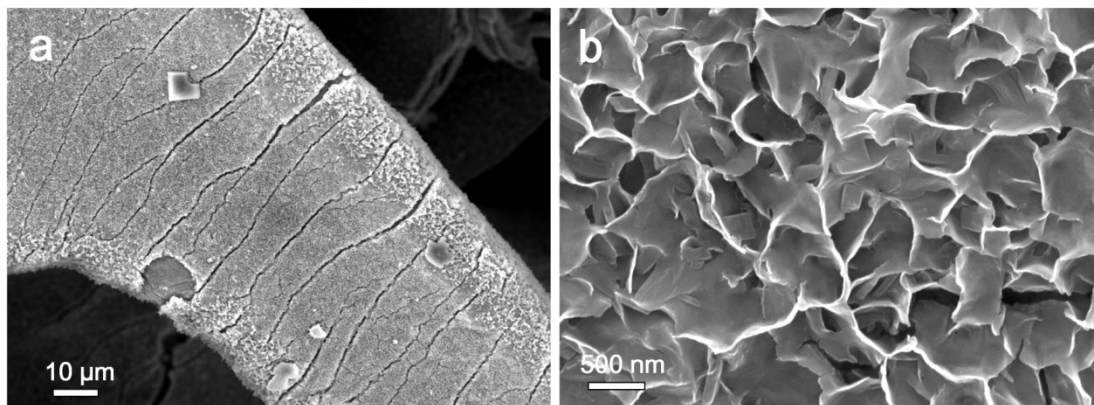


Fig. S7 SEM images of Ni_3S_2 electrode after 10 000 cycles in three-electrode system.

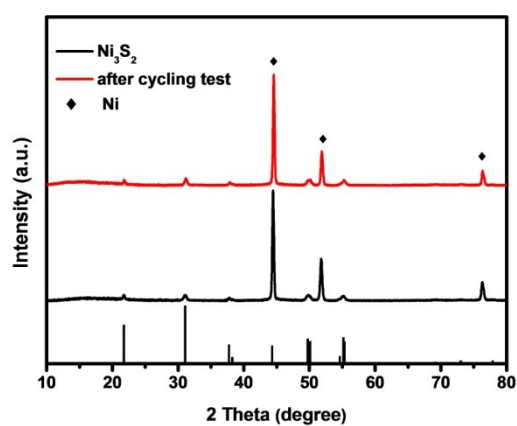


Fig. S8 XRD pattern of the Ni_3S_2 electrode before and after 10 000 cycles in three-electrode system.

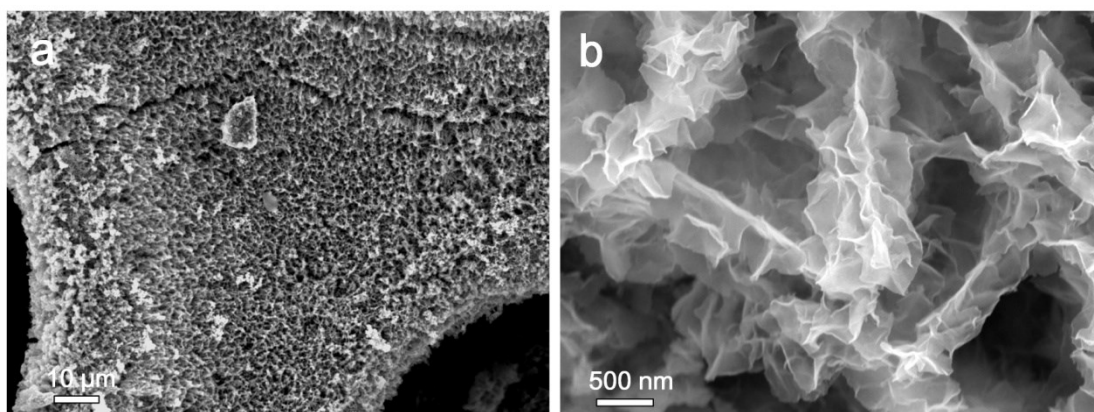


Fig. S9 SEM images of $\text{Co-Ni}_3\text{S}_2$ electrode after 10 000 cycles in three-electrode system.

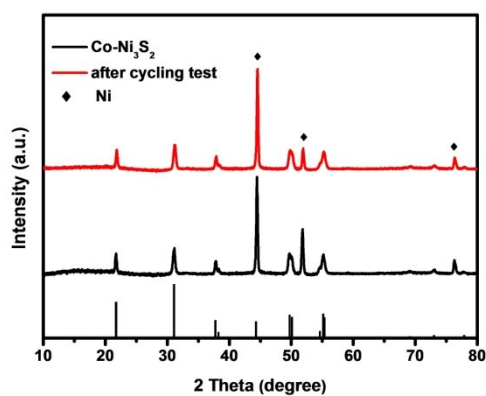


Fig. S10 XRD pattern of Co-Ni₃S₂ electrode before and after 10 000 cycles in three-electrode system.

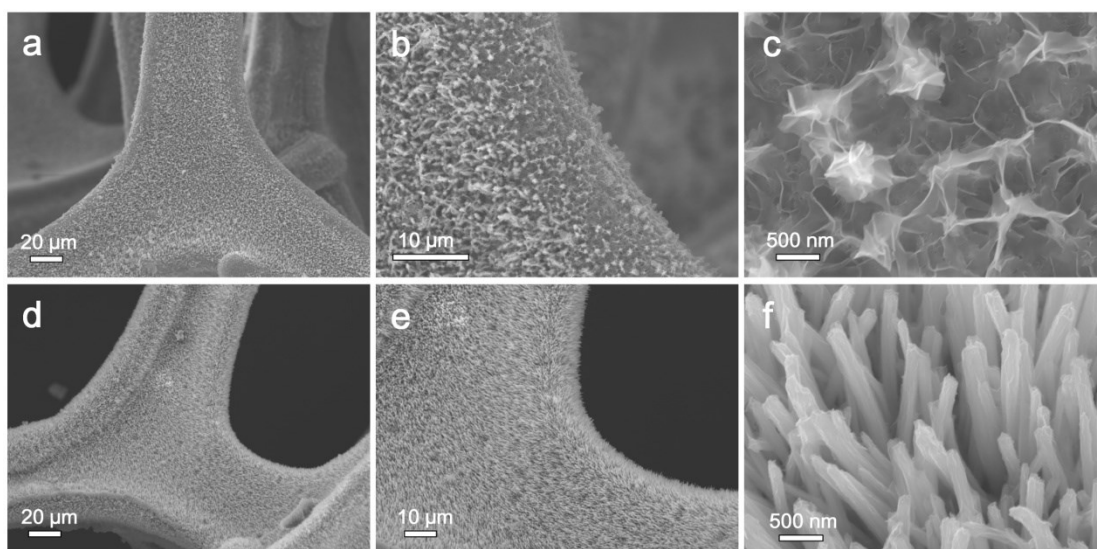


Fig. S11 SEM images of Co-Ni₃S₂ with different cobalt nitrate feeding amounts. (a-c) Co-Ni₃S₂-L; (d-f) Co-Ni₃S₂-H.

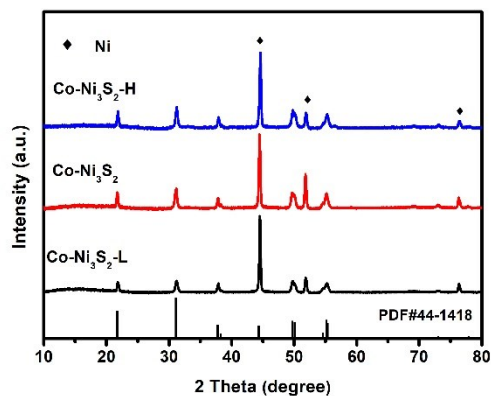


Fig. S12 XRD pattern of the Co-Ni₃S₂ with different cobalt nitrate feeding amounts.

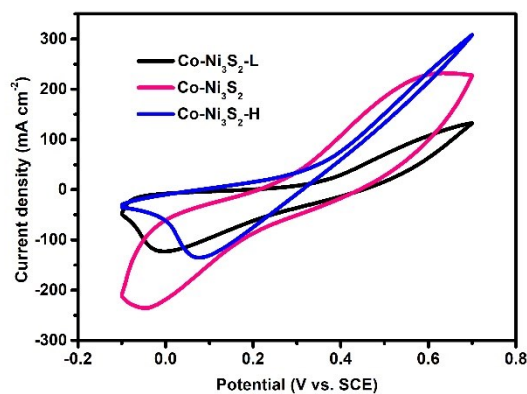


Fig. S13 CV curves of the Co-Ni₃S₂ with different cobalt nitrate feeding amount at a scan rate of 100 mV s⁻¹.

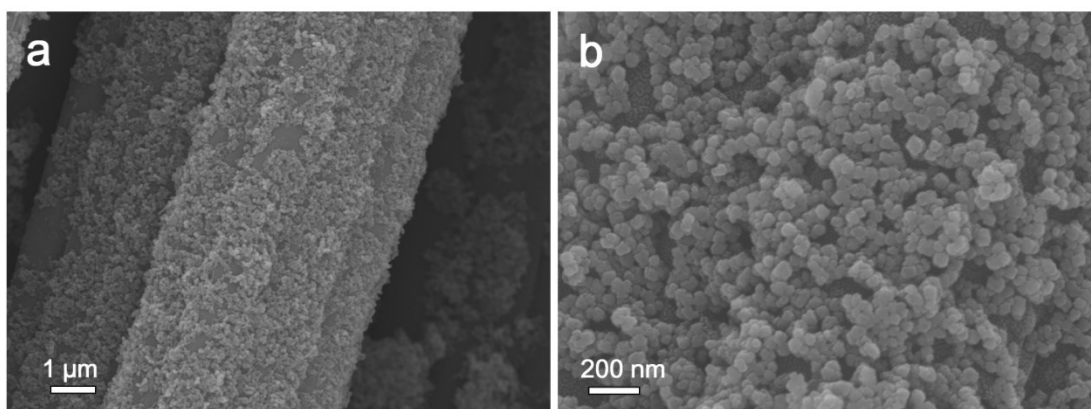


Fig. S14 SEM images of FeOOH nanoparticles at different magnification.

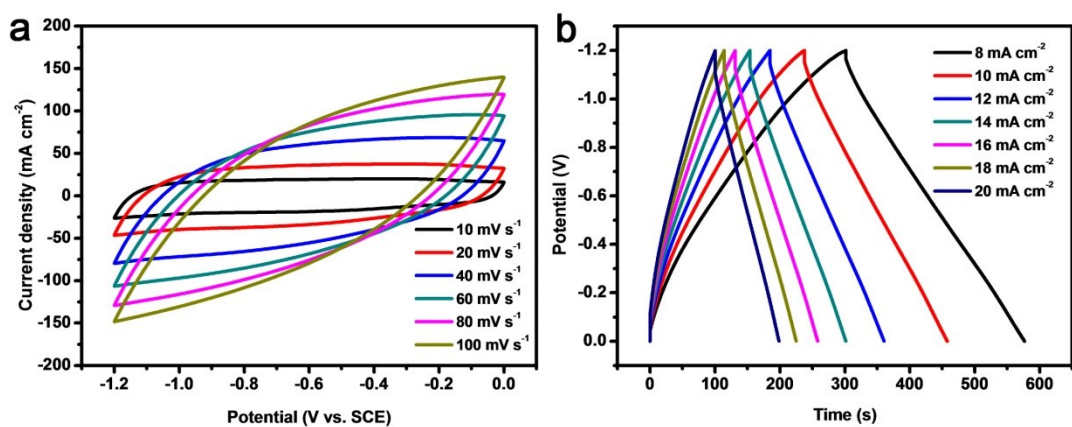


Fig. S15 Electrochemical performances of the FeOOH electrode. (a) CV curves collected at various scan rates, and (b) GCD curves collected at different current densities.

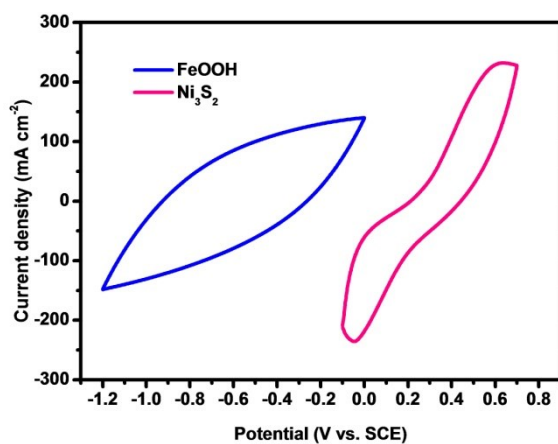


Fig. S16 CV curves of FeOOH and $\text{Co-Ni}_3\text{S}_2$ electrodes collected at 100 mV s^{-1} .

Table S2. Comparison of the electrochemical performances of Co-Ni₃S₂//FeOOH HSCs with recently reported state-of-the-art supercapacitors.

Electrode	Morphology	Current density) [mAcm ⁻²]	CP areal capacitance [Fcm ⁻²]	Substrate	Electrolyte	Reference
Co-Ni₃S₂//FeOOH	nanorods	10	1.61	NF	1.0 M KOH	This work
Ni ₃ S ₂ @CdS//C	nanorods	8	0.60	NF	3.0 M KOH	S1 ¹
Ni ₃ S ₂ @β-NiS//AC ^{c)}	nanosheet	4	0.08	NF	6.0 M KOH	S3 ³
Co ₃ O ₄ @C@Ni ₃ S ₂ //AC	nanoneedle	20	0.327	NF	3.0 M KOH	S5 ⁵
NF@NiO//FeOOH	nanosheet	8	0.527	NF	1.0 M KOH	S6 ⁶
Ni-Co-O//AC	nanosheet	15	0.517	NF	3.0 M KOH	S7 ⁷
Ni-Co-S//graphene	nanosheet	1.6	0.263	NF	1.0 M KOH	S8 ⁸

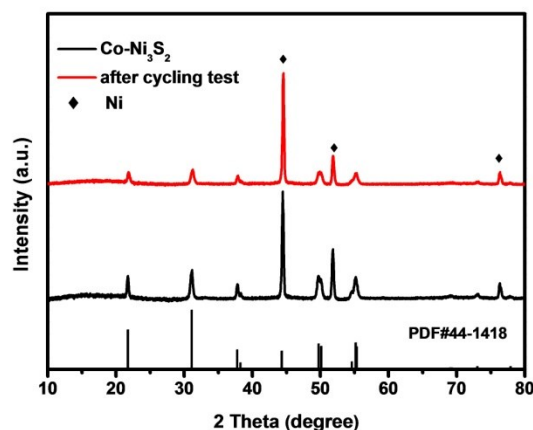


Fig. S17 XRD patterns of the Co-Ni₃S₂ electrode before and after 5 000 cycles in Co-Ni₃S₂//FeOOH HCSs.

Reference

1. X. Wang, B. Shi, Y. Fang, F. Rong, F. Huang, R. Que and M. Shao, *J. Mater. Chem. A*, 2017, **5**, 7165-7172.
2. N. Wang, X. Ma, H. Xu, L. Chen, J. Yue, F. Niu, J. Yang and Y. Qian, *Nano Energy*, 2014, **6**, 193-199.
3. H. Huo, Y. Zhao and C. Xu, *J. Mater. Chem. A*, 2014, **2**, 15111-15117.
4. M. Yu, W. Wang, C. Li, T. Zhai, X. Lu and Y. Tong, *NPG Asia Mater*, 2014, **6**, e129.
5. D. Kong, C. Cheng, Y. Wang, J. I. Wong, Y. Yang and H. Y. Yang, *J. Mater. Chem. A*, 2015, **3**, 16150-16161.
6. Q. Chen, J. Li, C. Liao, G. Hu, Y. Fu, K. A. Owusu, S. Shi, Z. Liu, L. Zhou and L. Mai, *J. Mater. Chem. A*, 2018, **6**, 19488-19494.
7. Y. Li, L. Cao, L. Qiao, M. Zhou, Y. Yang, P. Xiao and Y. Zhang, *J. Mater. Chem. A*, 2014, **2**, 6540-6548.
8. W. Chen, C. Xia and H. N. Alshareef, *ACS Nano*, 2014, **8**, 9531-9541.